Supplemental Info

Influence of metal-coordinating comonomers on the coordination structure and binding in magnetic poly(ionic liquid)s

Kayla Foley[1], Lucas Condes[2], Keisha B. Walters[1]*
[1] Ralph E. Martin Department of Chemical Engineering, University of Arkansas, Fayetteville, AR 72701
[2] School of Chemical, Biological and Materials Engineering, University of Oklahoma, Norman, OK 73019

Keywords: poly(ionic liquids), magnetism, paramagnetic, copolymer, industrial applications

Magnetic Video Characterization

Supplemental videos showing magnetic attraction are included as supplementary files. In each video, a magnet with a calculated surface field strength of 0.62 T was held close to the dry polymers or the [Pam-*co*-PDADMA][Fe^{3+}] and [Pam-*co*-PDADMA][Mixed Fe^{3+}/Co^{2+}] suspensions. Clear magnetic attraction was observed in all cases.

UV-Vis Spectra

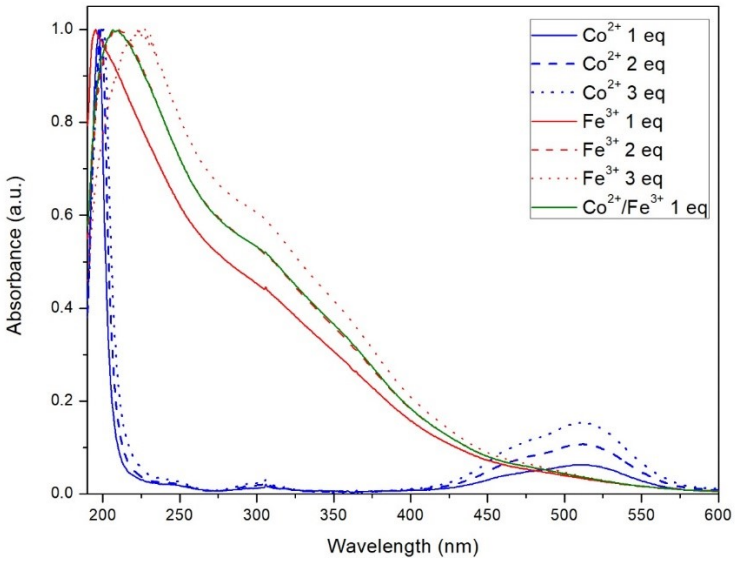

Figure S1. UV-visible spectra of the salts $CoCl_2$ (blue), $FeCl_3$ (red), and their mixtures in aqueous solution without any added copolymer.

ATR-FTIR Spectra

Table S1. ATR-FTIR frequencies of the amide N-H stretches, amide I, amide II, and metal hydroxide stretching and bending modes for the [Pam-*co*-PDADMA][X] copolymers where X indicates [Cl^-] anions or the transition metal salt complexes for each mole equivalence.

[Pam-*co*-PDADMA][X]	**Cl^-**	**Fe^{3+}**			**Co^{2+}**			**Mixed**			**Metal Halide Salts**	
Sample		**1eq**	**2eq**	**3eq**	**1eq**	**2eq**	**3eq**	**1eq**	**2eq**	**3eq**	**$CoCl_2*6H_2O$**	**$FeCl_3*6H_2O$**
N-H asym	3286	3330	3330	3330	3333	3333	3384[a]	3335	3335	3389[a]	3522, 3383, 3163[a]	3526, 3386, 3217, 3005[a]
N-H sym	3200	3190	3190	3190	3192	3196	3162[a]	3192	3192	3175[a]	--	--
Amide I (C=O str)	1662	1650	1643	1643	1656	1654	1648	1657	1650	1642	--	--
M-OH	--	--	--	1608	--	--	1620	--	--	--	1618, 1643[a]	1595[a]
Amide II (NH_2 wag)	1615	1574	1568	1565	1604	1599	1597	1607, 1572[b]	--	--	--	--
Amide III (N-C str)	1417	1417	1417	1417	1418	1417	1416	1418	1416	1416	--	--

[a] Peaks are related to the hydrated metal M-O-H stretch or bending modes overlapping with the amide modes.

[b] Peaks determined through peak deconvolution.

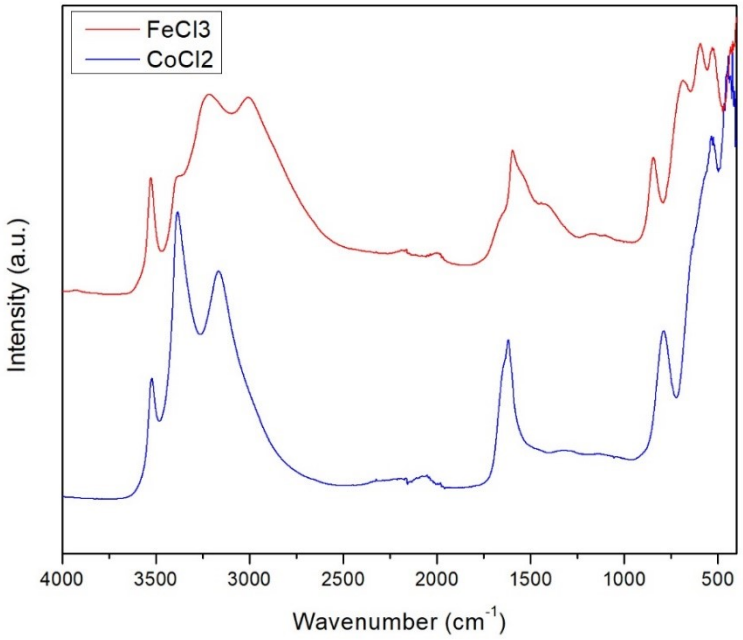

Figure S2. ATR-FTIR spectra of the $CoCl_2$ and $FeCl_3$ salts with no added polymer.

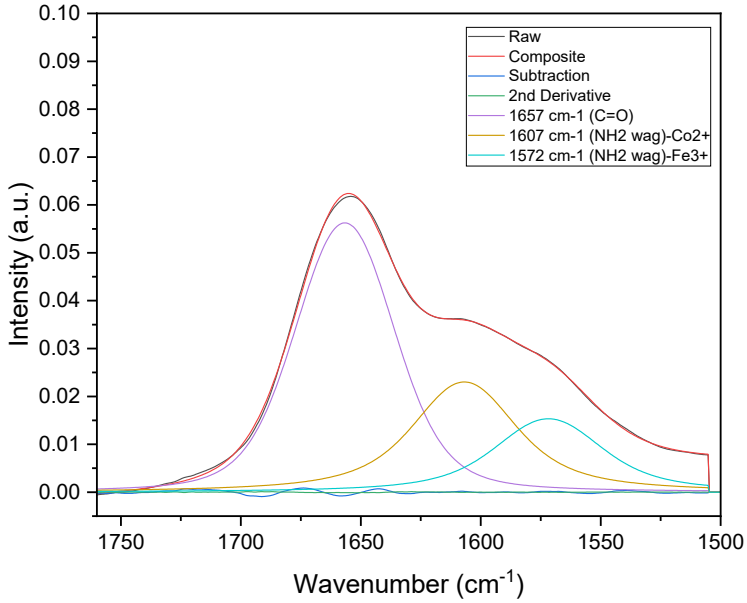

Figure S3. Deconvolution result of the amide region for the [Pam-*co*-PDADMA][Mixed Fe^{3+}/Co^{2+} 1eq] ATR-FTIR spectra. The peak centers are located at 1657 cm^{-1} (amide I C=O), 1607 cm^{-1} (amide II-Co^{2+}), 1572 cm^{-1} (amide II-Fe^{3+}).

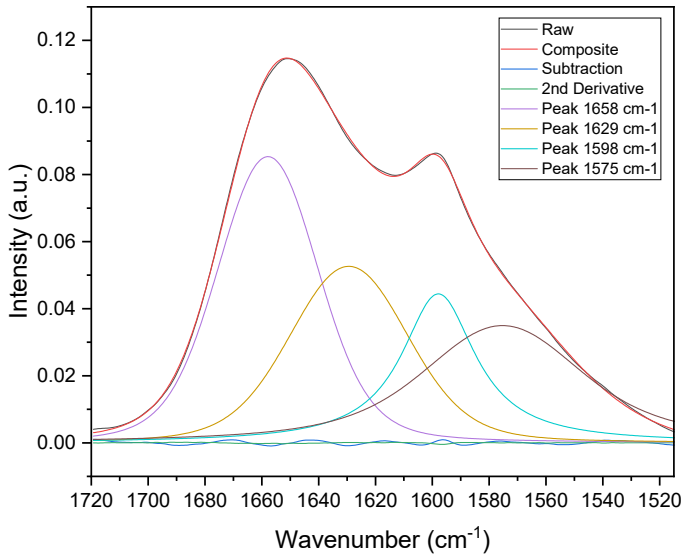

Figure S4. Deconvolution result of the amide region for the [Pam-*co*-PDADMA][Mixed Fe^{3+}/Co^{2+} 2eq] ATR-FTIR spectra. Two peaks were observed for amide I C=O (1658 and 1629 cm^{-1}) and two peaks for amide II NH_2 wag (1598 and 1575 cm^{-1}).

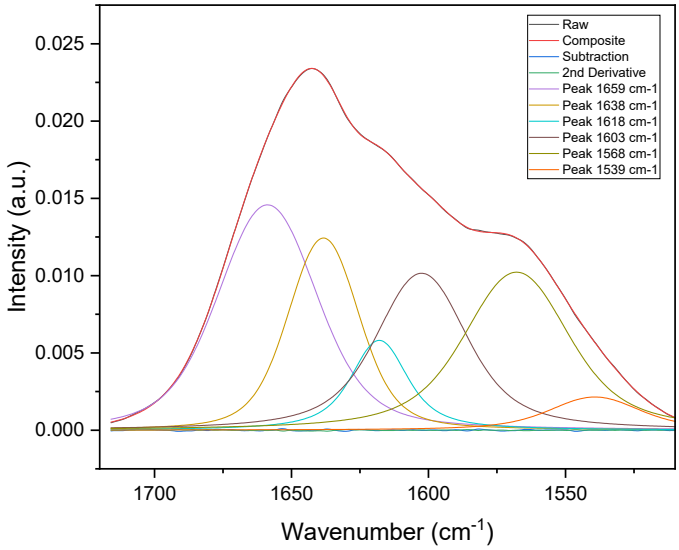

Figure S5. Deconvolution result of the amide region for the [Pam-*co*-PDADMA][Mixed Fe^{3+}/Co^{2+} 3eq] ATR-FTIR spectra. Two peaks were observed for amide I C=O (1659 and 1638 cm^{-1}) and two peaks for amide II NH_2 wag (1603 and 1568 cm^{-1}). The peak at 1618 cm^{-1} is likely Co-OH from excess uncoordinated salt.

XPS Spectra

Table S2 XPS peak positions (± 0.2 eV) and area percentages for collected high resolution spectra for the N1s, O1s, and C1s spectral ranges corresponding to the high resolution spectra shown in Figure 8.

	N1s						**O1s**								**C1s**					
	PDADMA		*Pam*		*Pam-M*		*Pam*		*M-O*		*Water*		*Na KLL*		*Aliphatic*		*PDADMA*		*Pam*	
Sample	Position	%	position	%	position	%	position	%	position	%	position	%	position	%	position	%	position	%	position	%
[Pam-*co*-PDADMA][Cl^-]	402.4	46.6	399.6	53.4	--	--	531.3	41.9	--	--	532.5	16.8	536.1, 538.0	41.4	285.0	55.2	286.1	33.3	287.7	11.5
[Pam-*co*-PDADMA][Co^{2+} 1eq]	402.4	45.0	400.0	55.0	--	--	531.9	94.5	--	--	533.6	2.0	536.1	3.5	285.0	55.2	286.1	39.6	288.5	5.3
[Pam-*co*-PDADMA][Co^{2+} 2eq]	402.6	44.8	400.2	27.6	402.1	27.6	532.3	83.7	--	--	533.5	12.2	536.3	4.0	285.0	55.2	286.2	43.1	288.8	1.7
[Pam-*co*-PDADMA][Fe^{3+} 1eq]	402.5	44.8	399.8	29.6	402.0	25.6	531.6	74.5	529.9	3.33	532.3	20.4	535.7	1.7	285.0	47.7	286.2	45.0	288.1	7.3
[Pam-*co*-PDADMA][Fe^{3+} 2eq]	402.5	44.8	400.0	37.4	402.3	17.9	531.8	88.3	530.1	9.96	533.3	1.8	--	--	285.0	55.7	286.3	37.9	288.6	6.4
[Pam-*co*-PDADMA][Mixed Fe^{3+}/Co^{2+} 1eq]	402.4	44.8	399.8	44.7	401.9	10.6	531.7	71.3	529.9	3.3	533.2	4.7	535.7	20.8	285.0	55.1	286.2	34.0	288.1	10.9

Table S3 XPS peak positions (± 0.2eV) for the Fe $2p^{3/2}$, Co $2p^{3/2}$, and Cl $2p^{3/2}$ peaks in the respective 2p high resolution spectra shown in Figure 8 of the main text.

	Metals		Cl $2p^{3/2}$		
Sample	Fe $2p^{3/2}$	Co $2p^{3/2}$	Main Species	Minor Species	Ref.
[Pam-*co*-PDADMA][Cl^-]	--	--	198.8	--	This work
[Pam-*co*-PDADMA][Co^{2+} 1eq]	--	781.6	198.4	--	This work
[Pam-*co*-PDADMA][Co^{2+} 2eq]	--	781.9	198.8	200.1	This work
[Pam-*co*-PDADMA][Fe^{3+} 1eq]	710.9	--	198.4	200.2	This work
[Pam-*co*-PDADMA][Fe^{3+} 2eq]	711.4	--	198.7	200.2	This work
[Pam-*co*-PDADMA][Mixed Fe^{3+}/Co^{2+} 1eq]	710.9	781.3	198.4	200.0	This work
$FeCl_3$	711.5		199.7		Grosvenor et al.[1]
$FeCl_3$, Russo et al.	712.0		199.0		Russo et al.[2]
$[Et_4N^+][FeCl_4]^-$	711.2		198.6		Russo et al.[2]
$[C_8C_1Im^+][FeCl_4]^-$	711.9		199.4		Taylor et al.[3]
$[C_8C_1Im^+][CoCl_4]^{2-}$		780.6	198.2		Taylor et al.[3]
$CoCl_2$		782.1			Brown et al.[4]

XPS survey spectra for all samples are shown below.

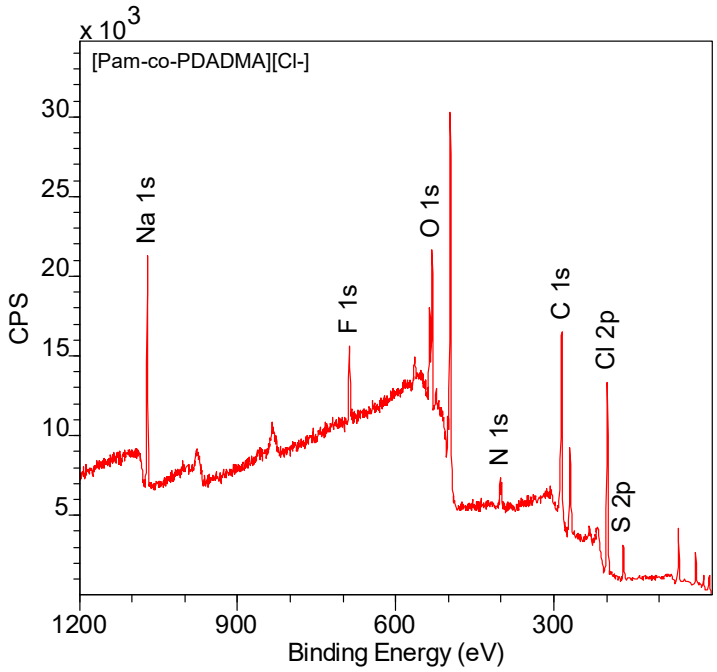

Figure S6. XPS survey spectrum for [Pam-*co*-PDADMA][Cl^-].

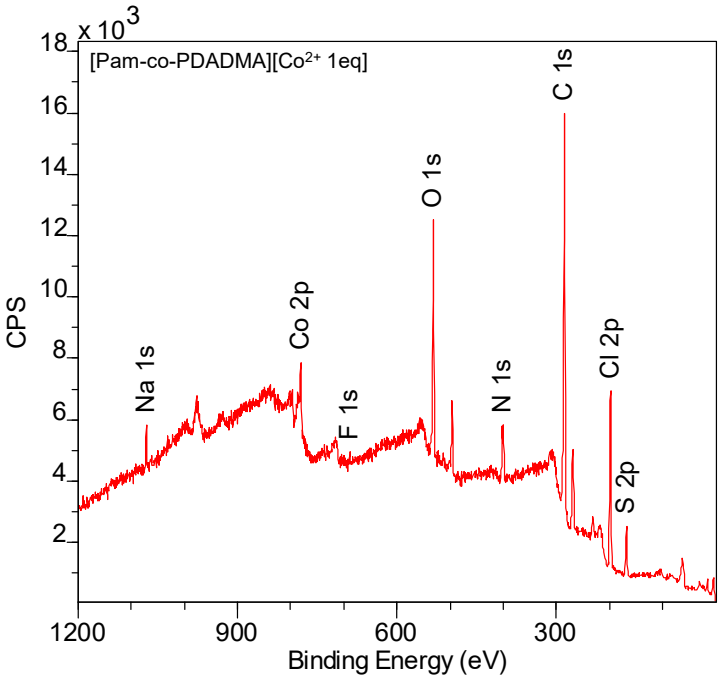

Figure S7. XPS survey spectrum for [Pam-*co*-PDADMA][Co^{2+} 1eq].

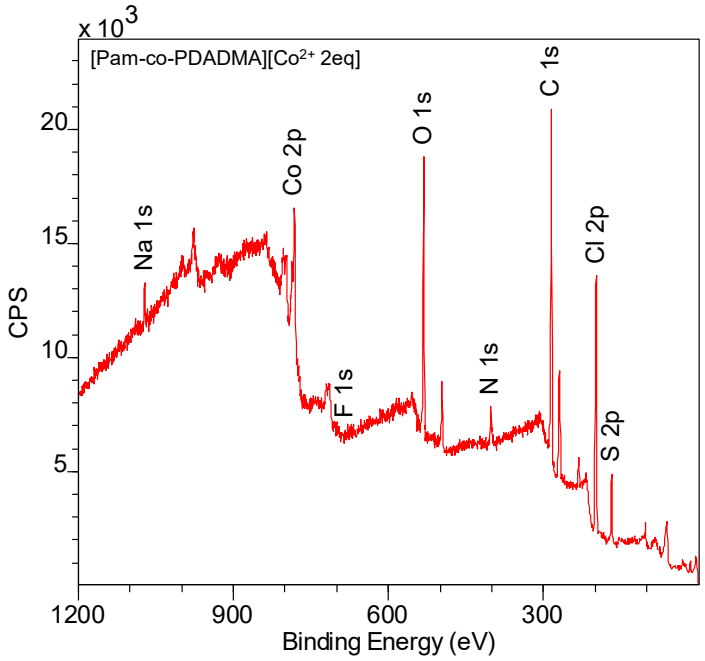

Figure S8. XPS survey spectrum for [Pam-*co*-PDADMA][Co^{2+} 2eq].

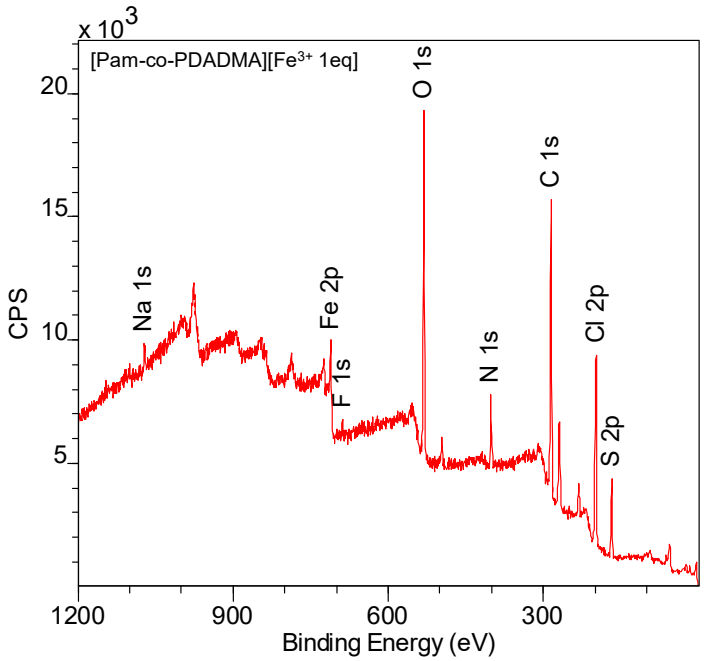

Figure S9. XPS survey spectrum for [Pam-*co*-PDADMA][Fe^{3+} 1eq].

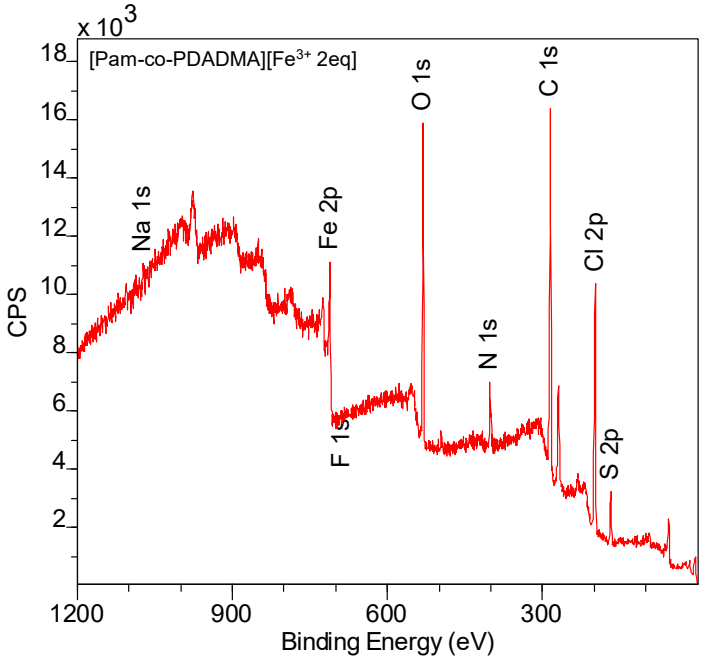

Figure S10. XPS survey spectrum for [Pam-*co*-PDADMA][Fe^{3+} 2eq].

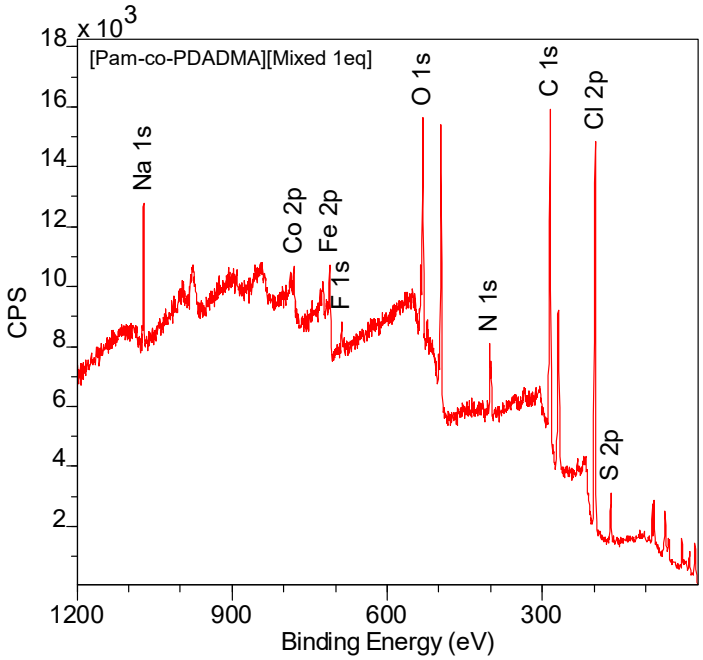

Figure S11. XPS survey spectrum for [Pam-*co*-PDADMA][Mixed 1eq].

Comparison of Metal Coordination in Polyacrylamide Homopolymer

Synthesis of Polyacrylamide. All materials and reagents were used as received from the vendor without any further purification. Ultrapure acrylamide monomer was purchased from VWR Life Science, potassium persulfate (radical initiator) was purchased from Fisher Scientific, and ultrapure type 1 water was prepared in-house by a Synergy® UV-R water purification system. Ultrapure acrylamide monomer (7.07 g, 99.5 mmol), ultrapure type 1 water (200 mL), and initiator potassium persulfate (69.6 mg, 0.259 mmol) were added to a three-necked round-bottom flask equipped with a reflux condenser. The reaction mixture was degassed by nitrogen sparge for 30 minutes before being heated to 45 °C in a water bath under stirring. The polymerization was performed for 2 h under stirring at temperature. The highly viscous reaction mixture was immediately precipitated into 500 mL of acetone, collected, redissolved into 200 mL of water, and then precipitated into a 400 mL of 3:1 acetone:water solution by volume, and then left under stirring for ten minutes. The isolated polyacrylamide product was collected and dried under vacuum at ambient temperature for 48 h.

ATR-FTIR Comparison of Polyacrylamide Homopolymer and the [Pam-co-PDADMA][Cl$^-$] Copolymer. The neat homopolymer poly(acrylamide) synthesized *via* conventional free radical polymerization was characterized using ATR-FTIR (Figure S12). A dried film of the neat poly(acrylamide) displayed amide I (C=O str) and amide II (NH_2 wag) bands at 1651 cm^{-1} and 1608 cm^{-1}, respectively. Compared to the unmodified commercial [Pam-*co*-PDADMA][Cl$^-$] copolymer used in the main study of this work, the amide I band was downshifted 11 cm^{-1} and the amide II band was downshifted 7 cm^{-1} in the poly(acrylamide) homopolymer.

The [Pam-*co*-PDADMA][Cl$^-$] copolymer is expected to have less intramolecular hydrogen bonding interactions occurring between the hydrogen bond donor (C=O) and acceptor (NH) in the amide groups occurring due to steric hinderance introduced by the diallyl dimethyl ammonium comonomer compared to the poly(acrylamide) homopolymer. The higher wavenumbers observed in the [Pam-*co*-PDADMA][Cl$^-$] copolymer for the amide I (C=O str) reflect this decrease in self-hydrogen bonding of the amide groups as a result of the shorter C=O bond compared to the longer C=O bond in hydrogen bonded -C=O···H_2N-. However, hydrogen bonding at the NH_2 group is expected to increase the frequency at which the Amide II (NH_2 wag) band occurs[5]. As the amide II band is found at a higher wavenumber in the copolymer compared to the neat poly(acrylamide) homopolymer, this suggests the NH_2 is receiving a hydrogen bond interaction from another other source. Tentatively, this hydrogen-bonding source is attributed to the Cl$^-$ counterions associated to the quaternary ammonium groups in the copolymer (R-NH_2···Cl$^-$) acting as a proton acceptor group.

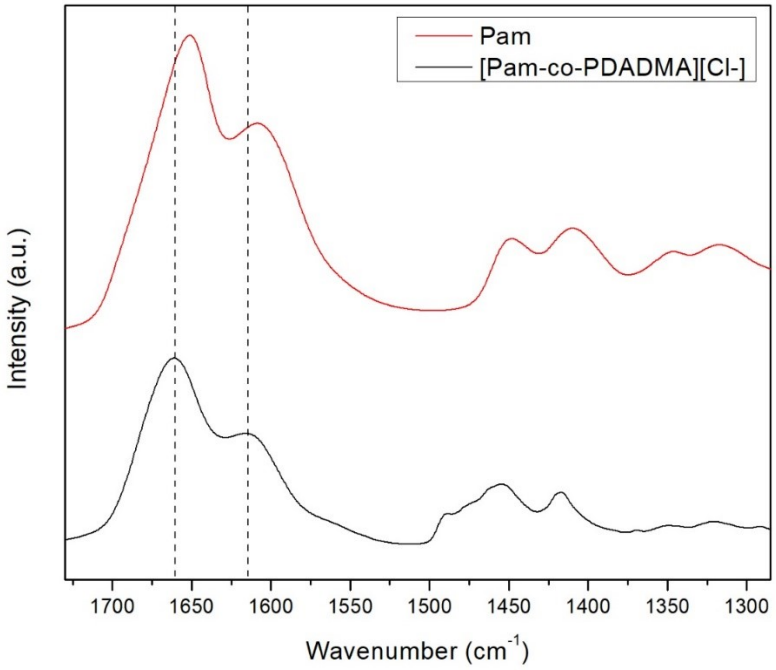

Figure S12. ATR-FTIR spectra of the poly(acrylamide-*co*-diallyl dimethyl ammonium chloride) copolymer and poly(acrylamide) homopolymer. The dotted lines indicate the observed shifts in the amide I and amide II bands.

Supplemental Info References

1. A. P. Grosvenor, B. A. Kobe, M. C. Biesinger and N. S. McIntyre, *Surface and Interface Analysis*, 2004, **36**, 1564-1574.
2. M. V. Russo, G. Polzonetti, A. Furlani, A. Bearzotti, I. Fratoddi and P. Altamura, *Journal of Vacuum Science & Technology A*, 1998, **16**, 35-44.
3. A. W. Taylor, S. Men, C. J. Clarke and P. Licence, *RSC Advances*, 2013, **3**, 9436-9445.
4. D. G. Brown and U. Weser, 1979, **34**, 1468-1470.
5. R. M. Silverstein and G. C. Bassler, *Journal of Chemical Education*, 1962, **39**, 546.